



UNIVERSITY OF LEEDS

This is a repository copy of *An Atomistic Analysis of the Carpet Growth of KCl Across Step Edges on the Ag(111) Surface*.

White Rose Research Online URL for this paper:

<https://eprints.whiterose.ac.uk/223177/>

Version: Accepted Version

Article:

Kny, A.J., Sweetman, A. orcid.org/0000-0002-7716-9045 and Sokolowski, M. (2025) An Atomistic Analysis of the Carpet Growth of KCl Across Step Edges on the Ag(111) Surface. *The Journal of Physical Chemistry Letters*, 16 (3). pp. 696-702. ISSN 1948-7185

<https://doi.org/10.1021/acs.jpcllett.4c02809>

This is an author produced version of an article published in *The Journal of Physical Chemistry Letters*, made available under the terms of the Creative Commons Attribution License (CC-BY), which permits unrestricted use, distribution and reproduction in any medium, provided the original work is properly cited.

Reuse

This article is distributed under the terms of the Creative Commons Attribution (CC BY) licence. This licence allows you to distribute, remix, tweak, and build upon the work, even commercially, as long as you credit the authors for the original work. More information and the full terms of the licence here:

<https://creativecommons.org/licenses/>

Takedown

If you consider content in White Rose Research Online to be in breach of UK law, please notify us by emailing eprints@whiterose.ac.uk including the URL of the record and the reason for the withdrawal request.



eprints@whiterose.ac.uk
<https://eprints.whiterose.ac.uk/>

An atomistic analysis of the carpet growth of KCl across Ag(111) step edges

Anna J. Kny,[†] Adam Sweetman,[‡] and Moritz Sokolowski^{*,†}

[†]*Clausius Institut für Physikalische und Theoretische Chemie, Universität Bonn, Bonn, 53115, Germany*

[‡]*School of Physics and Astronomy, University of Leeds, Leeds, LS2 9JT, United Kingdom*

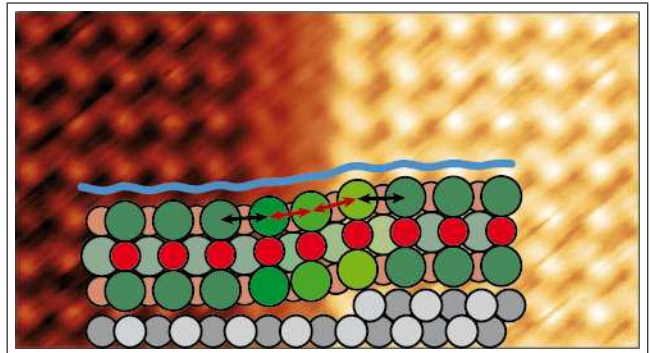
E-mail: sokolowski@pc.uni-bonn.de

Abstract

The carpet growth of alkali halide (AH) layers across step edges of substrates enables the growth of seamless and continuous large domains. Yet, information about how the AH layer adapts continuously to the height difference between the terraces on the two sides of a step are only described by continuum models which do not give details of the ionic displacements. Here, we present a first study on thin epitaxial KCl(100) layers grown on the Ag(111) surface by scanning tunneling microscopy that provides atomistic details for the first time. Measurements were performed at room temperature. Using a Cl^- -decorated tip, we resolved the ionic arrangement and hence the KCl lattice distortion in the carpet growth region, in some cases even by imaging both types of ions. Our findings demonstrate the ability of the KCl lattice to distort locally over a short distance of four KCl unit cells as a result of the attractive interaction between the ions and the Ag atoms at and close to the steps. For Ag step edges covered by the KCl carpet, we observe a tendency to straighten along the $\langle 110 \rangle$ direction of the KCl layer. In addition, the carpet growth induces the formation of Ag microterraces, i.e., the splitting of higher Ag steps into multiple Ag steps of mono-atomic height during the KCl deposition at elevated temperatures. These microterraces have a minimum width determined by an energetically preferred

fitting to the KCl lattice and allow for the carpet growth, while growth across higher Ag steps is not observed.

TOC Graphic



Keywords

alkali halides; carpet growth; KCl; scanning tunneling microscopy (STM); tip modification at room temperature

Due to their wide bandgap, alkali halides (AH) offer the opportunity to grow epitaxial, super thin dielectric layers on metal surfaces. While layers of usually just two to three monolayer thickness are still thin enough to allow for electrons to tunnel through, they successfully prevent a hybridization of orbitals of adsorbed molecules with the electronic states of the underlying metal substrate.¹⁻³ For this reason AH films are widely used to study the properties of electronically decoupled molecules and their aggregates by scanning tunneling and also by atomic force microscopy.³⁻⁷ A controlled growth of the AH layers is important in order to achieve sufficiently closed and ordered films and hence the aspired properties. However, the lattice mismatch between the AH and the substrate surface causes a non trivial growth situation which strongly depends on the specific material combination. For many combinations of AH and substrates, a growth behavior called *carpet* growth is observed that allows for a seamless growth of AH domains across steps of the substrate.⁸⁻¹⁵ Existing models for the carpet growth use a continuum description from elasticity theory for the AH layers in which the specific ionic positions are unresolved.^{8,10} However, as AH ions interact with local charges at metal step edges,^{14,16,17} distortions of the AH films at step edges are likely. Hence, a continuum model is expected to provide only a coarse approximation for the situation.

In this letter we present a detailed atomistic model for the carpet growth of KCl(100) on the Ag(111) surface which shows that a lattice distortion is indeed present and that it is concentrated in two out of four KCl unit cells in the carpet region at the steps. The ion positions were derived from STM measurements with extremely high atomic resolution. We describe the growth across single, double, and triple steps of the Ag substrate. Two surprising features are seen for Ag step edges which are overgrown by KCl: (i) Higher Ag steps (e.g., double or triple steps) split into mono-atomic steps, and (ii) step edges rearrange in their direction such that they follow the polar $\langle\bar{1}10\rangle$ KCl lattice lines on a local scale. The originally

energetically unfavorable situation at the step edge hence changes to one in which both the KCl lattice and the Ag surface adapt to each other, favoring attractive interactions between the ions and the step dipoles.

The major reason for the occurrence of carpet growth is that the AH film exhibits a different height for a mono-atomic layer (ML) than the substrate material. Thus, for AH films thicker than 1 ML, the vertical offset caused by a mono-atomic substrate step leads to repulsive Coulomb interactions between the ions on the upper and lower terrace at the step. This offset is avoided by the continuous carpet growth. It was first observed for the growth of NaCl(100) layers on the semiconductor surface Ge(100) by Schwennike et al.⁸ Using a continuum model for the AH layer, it was explained how the AH film grows seamlessly across substrate steps and adapts to the new terrace height like a uniform carpet.⁸ In this model, the strained carpet regions connect the undistorted domains on the upper and lower substrate terraces and extend laterally and vertically over many unit cells.⁸ This keeps the unfavorable vertical bending of the AH layer, which would otherwise create repulsive Coulomb forces, small, but only at the expense of a loss of interfacial binding energy in the areas close to the steps in which the AH film is detached from the Ge surface.⁸

STM measurements on AH films of thicknesses up to three atomic layers have reported widths for the strained carpet region of 25 Å for NaCl/Ge(100),¹⁸ 15.7 Å for NaCl/Ag(100),¹⁰ and 8 Å for NaCl/Ag(111).¹⁴ Assuming a surface lattice constant of $a_{\text{NaCl}} = 1/\sqrt{2} \cdot a_{\text{bulk}} = 3.99$ Å,¹⁹ this implies that the strain in the AH layer is distributed over a length of two to six surface unit cells in the direction perpendicular to the substrate step edge. Furthermore, a strain in the direction parallel to the step edge could also be present, but was not resolved yet. A film thickness dependent width of the carpet region was found by low energy electron diffraction measurements for NaCl/Ge(100)⁸ and NaCl/Ag(100).¹⁰ The increase of the width of the carpet regions with the layer thickness

indicates a gradient of the lattice distortion of the AH layers in the vertical direction.

Considering the carpet growth on metal surfaces, the "smearing out" of the electron density at step edges, leading to the Smulochowski dipole, also needs to be considered. It can influence the ionic arrangement at the step edge. The electron density excess at the lower step edge site and the depletion at the upper one²⁰ promote a growth mode with the polar $\langle \bar{1}10 \rangle$ direction of AH domains parallel to the step edge.¹⁷ This is evidenced by the observation that domains often nucleate at step edges,^{14,15,21} either on the upper or the lower step edge site, although this does not rigorously exclude a growth starting at defects on terraces. A growth starting at steps is also found for AH layers growing on-top of a 2 ML thick wetting layer as, e.g., reported for KCl/Ag(100).^{11,21} Due to the favored adsorption sites created by the Smulochowski dipole and the resulting ion arrangement on the upper and lower step edge sites, multilayer AH domains have the same azimuthal orientation on the upper and lower terrace. This promotes the seamless overgrowth of the steps and induces the carpet growth.

For the present reported experiments, sample preparation and measurements were performed in ultra high vacuum at a base pressure of $2 \cdot 10^{-10}$ mbar. The Ag(111) crystal was cleaned by sputtering with argon ions (10^{-5} mbar argon, 1 kV beam energy, 5 mA emission current) and subsequent annealing at about 820 K. The KCl (purchased from VWR, >99.5%, degassed in UHV) was deposited from a Knudsen cell at 853 K while the sample was kept at an elevated temperature of 403 K (± 5 K). Mühlpointner et al. found that this temperature is the optimal one for gaining a minimum of remaining bare Ag surface for growth of KCl on Ag(100).²² All measurements were performed at room temperature using a tungsten tip on a ScientaOmicron VT-STM/AFM with a Nanonis controller. Given bias voltages (U_{bias}) refer to the sample. Images were recorded in constant current (I_t) mode.

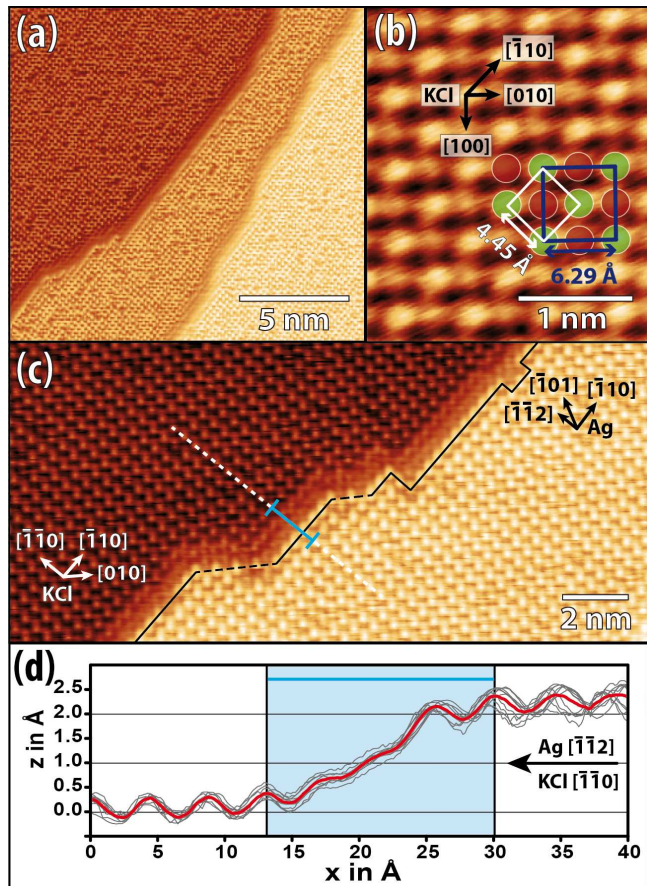


Figure 1: (a) Overview STM image of a KCl layer of 3 ML height which grows across two Ag steps of mono-atomic height. (b) STM image of a 2 ML KCl layer showing the positions of both ions superimposed by a hard sphere model ($U_{\text{bias}} = -1.684$ V, $I_t = 3$ nA). The STM image was measured at a different sample region than (a) and (c). The projected KCl bulk unit cell (dark blue), the smaller KCl surface unit cell (white) and the lattice directions of KCl are indicated. Color code: Cl^- (green spheres), K^+ (red spheres). (c) Magnification of the step edge area of (a) and indicated lattice directions for KCl and Ag. Higher terraces are indicated by brighter color. As demonstrated by the white dotted line, no lateral shifts are observed between the domains on the upper and lower Ag terrace. (d) Scatter plot (gray) and averaged line profile (red) measured along the $\text{KCl}[\bar{1}\bar{1}0]$ lattice direction across the mono-atomic Ag step visible in (c). In (c) and (d), the width of the carpet region is indicated by the solid line in light blue. ($U_{\text{bias}} = -1.3$ V, $I_t = 0.56$ nA). For further details, see text.

We start by giving some general details about the growth of KCl on Ag(111) before we focus on the carpet growth. Monolayer thick wetting layers are rare for AH,^{16,23} as these would require stronger compensation of the ionic charges by the respective mirror charges of the metal surface, compared to AH bilayers. We exclusively observed two layer thick wetting layers of KCl on Ag(111) for an overall coverage of about 2.5 ML that was chosen for our experiments. In addition, we observed partly a third layer on top of the wetting layer. Examples for 3 and 2 ML KCl layers are shown in Figure 1 (a) and (b), respectively. The KCl domains were of up to few hundreds of nm in size. Rare patches of uncovered Ag(111) surface were used to determine the layer thickness. Although the geometric single layer thickness derived from the 3D bulk unit cell is 3.15 Å,^{19,24-27} measured layer heights are far below the geometrically expected one due to the dielectric character of KCl. For measurements in constant current mode, this causes that the tip is less retracted from the surface for every additional KCl layer. As will be discussed later, this leads to different image contrasts for different layer heights of the AH film. We obtain 2.94 ± 0.04 Å for the height of KCl bilayers with respect to the Ag surface, while we measure a height of 1.66 ± 0.01 Å for a third mono-atomic layer grown on top of a bilayer. This is in agreement with earlier reports for KCl on Ag(100).²⁸

As mentioned above, an atomistic analysis of the carpet growth requires knowledge about the ionic positions in the carpet region and hence a very high resolution of STM measurements. Thus, we now comment on the STM resolution and contrast that we achieve by using decorated W-tips. Figure 1 (a) shows an overview STM image with two mono-atomic Ag steps which are overgrown by a KCl domain of 3 ML height. For better visibility, Figure 1 (c) shows a zoom-in on the ion arrangement at the Ag step edge. From STM measurements reported for metallic and Cl⁻ decorated W-tips,²⁹ we conclude that the bright protrusions observed in our STM images correspond to the positions of the Cl⁻ ions. Interestingly, for one set of

tunneling parameters, we were able to image both, the K⁺ and the Cl⁻ ions simultaneously, for KCl bilayers, as shown in Figure 1 (b), and partly for the carpet growth regions of 3 ML domains as it is visible in Figure 1 (c). In our measurements, this type of image contrast was reproducible and stable.

To date, the simultaneous imaging of anions and cations was only observed in rare cases, e.g., by Lauwaet et al.¹³ for NaCl/Au(111), and only for low temperatures of 4 K. To the best of our knowledge, we report the first measurements of this kind at room temperature. The difficulty for imaging both type of ions is that tunneling with a metallic W-tip through its $d_{x^2-y^2}$, p_z , or s -orbitals, which all interact with the Cl⁻ p_z -orbitals of the KCl layer, does not offer the spatial resolution needed.²⁹ This suggests that the W-tip in our measurements was decorated by an adsorbed Cl⁻ anion. This type of tip decoration was analyzed for NaCl/Au(111) by Li et al.²⁹ who found that the imaging of either Na⁺ or Cl⁻, or of both ions simultaneously can be achieved for different tip-sample distances and hence by an appropriate choice of the tunneling parameters. We achieve the same variation of the contrast when we keep the tunneling parameters constant but measure on AH films of different thicknesses. This can be derived from line profiles extracted from the image of Figure 2 (c) (displayed in Figure S1 of the supporting information (SI)). These show a much higher atomic corrugation for the Cl⁻ ions of the third layer (52.7 ± 2.6 pm) compared to those in the KCl bilayer (14.7 ± 1.8 pm). The reason for this is that the overlap between the Cl⁻ p_z -orbital of the tip and the p_z -orbitals of the ionic layer increases when the tip-sample distance is decreased, as it occurs for tunneling on the third layer for the same I_t setpoint.²⁹ Because of this increased contrast for 3 ML KCl domains we focus on these to study the carpet growth.

In Figure 1 (c), the polar $\langle \bar{1}10 \rangle$ and non-polar $\langle 010 \rangle$ KCl lattice lines mentioned above are indicated by solid and dotted black lines, respectively. As expected from the orientation

effect related to the Smulochowski dipole, we find that the domains on the different terraces displayed in Figures 1 (a) and (c) have the same orientation, and we observe large sections in which the Ag steps run parallel to the polar $\langle \bar{1}10 \rangle$ lattice lines of the KCl layer. The AH layer thickness of 3 ML on both sides of the mono-atomic Ag step is hence an example of a situation in which carpet growth is expected to occur. An experimental evidence for this is that we find Cl^- ions of intermediate height contrast for four unit cells, marked by the light blue solid line in Figure 1 (b), in the region attached to the Ag step. A respective line profile is displayed in Figure 1 (d). This shows that the KCl film is vertically lifted from the lower terrace in a region close to the step edge, which we consider as the carpet region in the following. We note that we describe the exact positions of the ions in the carpet region below.

Before this, we discuss the fact that the KCl lattice is laterally strained due to the carpet growth and its possible impact. From the values of the bulk structure unit cells which are at 25°C $4.0856 \pm 0.0020 \text{ \AA}$ for Ag^{19,30-32} and $6.2915 \pm 0.0036 \text{ \AA}$ for KCl,^{19,24-27} we expect the KCl(100) surface lattice constant ($1/\sqrt{2} \cdot a_{\text{KCl}} = 4.45 \text{ \AA}$) to be 1.54 times larger than the Ag(111) surface lattice constant ($1/\sqrt{2} \cdot a_{\text{Ag}} = 2.89 \text{ \AA}$). For clarity, the, on the KCl(100) surface projected KCl bulk unit cell (dark blue) and the KCl(100) surface unit cell (white) are indicated in Figure 1 (b). For the KCl(100) lattice on the terrace but in a range of 15 nm adjacent to the strained carpet growth region, we obtained lattice constants of $4.29 \pm 0.06 \text{ \AA}$ parallel to the Ag step edges and a lattice constant of $4.34 \pm 0.07 \text{ \AA}$ perpendicular to the Ag step edges. For a detailed description of the determination method and comments about the errors, we refer to the SI. The difference of 1% between the two lattice constants is within the error range of our measurements and should be considered with care. However, the contraction of about 3% compared to the bulk derived lattice constant (4.45 \AA) is beyond the error range, and hence we consider this to be a result of a lateral distortion of the KCl

lattice on the Ag(111) surface. The contraction is surprising as it causes stress in the ionic layer.

In the following we draw some conclusions on a possible commensurability of the KCl lattice to the Ag(111) surface in the directions parallel and perpendicular to the Ag steps. The discussion of a possible commensurability is motivated because this may be partly the driving force for the observed lateral contraction of the KCl lattice. Parallel to the steps, the polar KCl $[\bar{1}10]$ lattice direction is parallel to the Ag $\langle \bar{1}10 \rangle$ lattice line. In this direction, a commensurate growth of second order would be possible for a KCl lattice constant of 4.33 \AA which is within the error range of the measured lattice constant ($4.29 \pm 0.06 \text{ \AA}$). This would favor a straightening of the Ag step edges along the KCl $[\bar{1}10]$ direction, as observed in our measurements. For a respective model, we refer to Figure 3 (c), below.

In the direction perpendicular to the Ag steps, the $[\bar{1}\bar{1}0]$ direction of the KCl lattice is parallel to the Ag $\langle \bar{1}\bar{1}2 \rangle$ lattice line (s. Fig. 1 (c)). As the periodicity of the Ag lattice in the $\langle \bar{1}\bar{1}2 \rangle$ direction can be described by a lattice constant of $\sqrt{\frac{3}{2}} \cdot a_{\text{Ag}} = 5.00 \text{ \AA}$ (cf. Fig. 3 (c)), a commensurate KCl growth of 8th order could occur on the terraces for a KCl $[\bar{1}\bar{1}0]$ lattice constant of 4.38 \AA . This would be within the error range of our measurements, but due to the high order of commensurability, we expect only a low impact on the orientation of the KCl domains.

However, a mono-atomic Ag step causes a shift between the Ag terraces which equals one row of Ag atoms in the $\langle \bar{1}\bar{1}2 \rangle$ direction. This shift ($0.5 \cdot \sqrt{\frac{3}{2}} \cdot a_{\text{Ag}}$) decreases the order of commensurability perpendicular to the steps from 8th to 4th, but only for the carpet growth region, connecting both Ag terraces. This might hence explain, why the width of the carpet region equals four KCl unit cell in our experiments. Furthermore, it might be an additional reason for the lateral distortion in the carpet growth region on which we report below. As an interim summary, we state that a commensurate

growth parallel to and to some extent also perpendicular to the Ag steps may play a role for the observed lattice contraction and width of the carpet region.

Beside the growth across Ag single steps discussed so far, the carpet growth also proceeds across higher Ag steps which we will discuss now. As an example, Figures 2 (a) and (b) show a Ag double step which is partly overgrown by a KCl layer of 3 ML height. Figure 2 (c) shows a Ag triple step overgrown by both, a KCl bilayer (left side), and a KCl triple layer (right side). In Figure 2 (a), we observe a wetting layer of 2 ML thickness on the upper terrace, which is partly covered by a third layer. The white crosses in Figure 2 (a) indicate the polar directions of the KCl lattice and thus the domain orientations. The third layer grows in registry with the wetting layer and no change in the orientation is observed. Furthermore, as indicated by the white dotted line, this domain grows across the Ag double step and continues on the lower Ag terrace without a lateral shift. The carpet region is indicated by a solid line in light blue. The two adjacent KCl domains on the lower Ag terrace of Figure 2 (a), on the other hand, do not overgrow the Ag double step as evident from their different orientations. As most KCl domains start growing at Ag steps, which are in $\langle \bar{1}\bar{1}0 \rangle$ orientation, angles between KCl domains on Ag(111) are found to be multiples of 30° .

Figure 2 (b) shows a magnification of the carpet growth region of Figure 2 (a) and respective line profiles given as a scatter plot. As Figure 2 (a) reveals, we observe that the double step is maintained as a (not split) double step for those regions where it is not overgrown by a KCl carpet, but where it only constitutes a boundary of the KCl domains. This is important because higher Ag steps which are overgrown by a coherent KCl domain generally split into multiple single steps. This splitting is indicated by the black markers on the light blue lines indicating the carpet region in (b) and (c). The so formed micro-terraces between two monoatomic Ag steps are of about 13 \AA in width.

This equals the width of three KCl unit cells and hence also the number of KCl unit cells in the carpet region of a single step minus one (see above). An example for the growth across a Ag triple step and respective line profiles is shown in Figure 2 (c). Although, we observe kink sites and hence changes in the course of the step, the micro-terraces never have a width of less than 13 \AA . Thus, we can conclude that a carpet growth on Ag(111) only exists for monoatomic Ag steps. In case of higher Ag steps, i.e., double and triple steps, the Ag steps split and form micro-terraces which allow for the carpet growth. We assume that this step splitting occurs during the KCl deposition at the elevated sample temperature (403 K).

To obtain an atomistic structure model for the strained carpet region, we analyzed profiles measured along the polar KCl $\langle \bar{1}\bar{1}0 \rangle$ direction perpendicular to Ag single and triple steps. These are shown in Figures 3 (a) and (b). The data is displayed as averaged profiles (red lines) of at least six individual scans and compared to hard sphere models. The respective scatter plots are displayed in Figure 1 (d) and 2 (c). Coordinates (x,z) of the Cl^- ions are directly derived from the maxima in the profiles. This assumes that electronic effects at the step edge have only a minor influence on the height profile. Cl^- ions on the terraces are displayed by a dark green color. For better visibility, the Cl^- ions in the carpet region are indicated by different green shades. As we cannot derive the positions of the underlying Ag step edges from the STM profiles, the structure models show Ag positions which are compatible with those of the KCl ions. Furthermore, when we compare the carpet growth for a 2 ML and 3 ML thick KCl layer, we can exclude a coverage dependent broadening of the carpet regions (s. Fig. 2 (c)). From this, we can conclude that, to adapt to the height of the next terrace, the ions in a KCl film shift vertically against each other (z direction), but that we do not have a gradient of the lattice distortion between the individual KCl layers.

As already described above, we observe a width

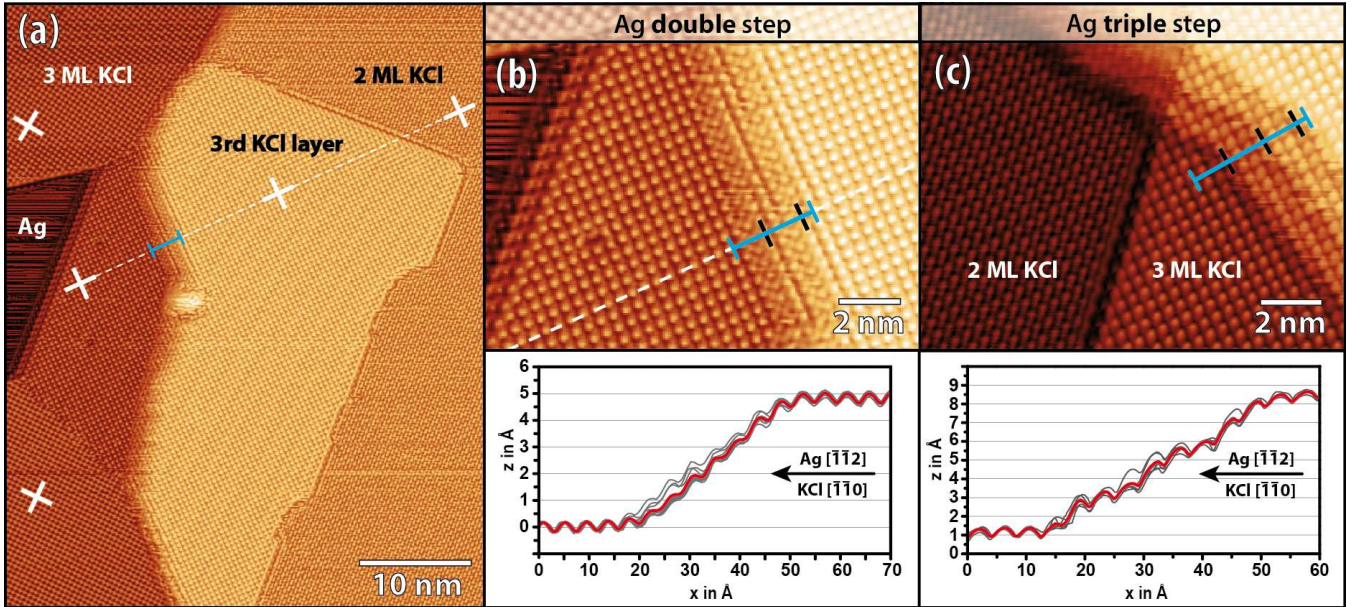


Figure 2: (a) Overview STM image showing different rotational domains of KCl beside bare Ag patches on the lower terrace (left side) and a KCl layer of 3 ML height growing from the upper terrace across the Ag double step in a carpet like growth mode. Domain orientations are indicated by white crosses, which lines follow the polar lattice lines of KCl. In (a), (b), and (c), the carpet width is indicated by a blue solid line. (b) STM image and line profiles showing the carpet growth across the split Ag double step displayed in (a). The KCl layer is of 3 ML thickness. (c) STM image and line profiles showing the growth of a KCl layer across a Ag triple step. The image was taken at a different sample region than (a). The KCl layer on the left side is of 2 ML thickness, the layer on the right side of 3 ML. Step and height indication as above. In (b) and (c), micro-terraces are indicated by gray markers along the blue solid line indicating the carpet width. Line profiles are given as a scatter plot with the averaged data displayed in red. $U_{\text{bias}} = -1.684$ V, $I_t = 3$ nA.

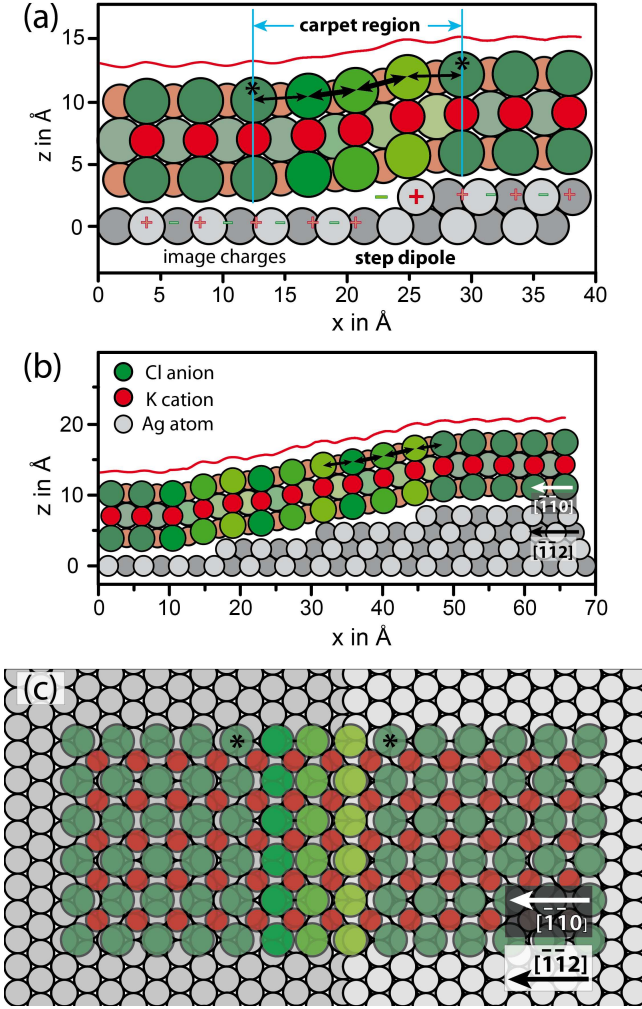


Figure 3: Averaged STM height profiles (red line) and hard sphere models of the carpet growth of a 3 ML KCl layer measured along the KCl $[\bar{1}\bar{1}0]$, and accordingly the Ag $[\bar{1}\bar{1}2]$, direction across a mono-atomic Ag step (a) and across a Ag step of 3 layer height with induced micro-terracing (b). Color code as indicated. Atoms in the background are indicated by fainter (K/Cl) or darker (Ag) color. Different green shades highlight Cl^- ions in structurally similar positions within the carpet region. Thick and thin black arrows indicate exemplary stronger and less strained unit cells in the carpet region, respectively. In (a) the the step dipole and the image charges are indicated. $U_{\text{bias}} = -1.684$ V, $I_t = 3$ nA. The vertical offset of the profiles with respect to the models is subject to some arbitrariness. The top view (c) refers to the mono-atomic Ag step illustrated in (a) on a reduced scale. The star symbol marks similar adsorption sites of the Cl^- ions adjacent to the carpet region.

of the carpet region of four KCl unit cells for the growth across a Ag single step, as shown in Figure 3 (a). Surprisingly, we find that the strain, induced to the KCl layer when it needs to adapt to the new terrace height, is not distributed uniformly across the KCl unit cells in the carpet region. A mono-atomic Ag(111) step has a height of 2.36 Å which needs to be overgrown. The unit cells adjacent to the upper and lower terrace compensate for 11% and 16% ($\pm 4\%$) of the height difference Δz (thin arrows in Fig. 3 (a)), while the two unit cells marked by thick arrows compensate 51% and 23%, respectively ($\pm 3\%$). This height difference of the Cl^- ions is accompanied by a lateral distortion Δx of the KCl unit cells in $[\bar{1}\bar{1}0]$ direction. Again, the distortion is not distributed uniformly across the carpet region. The minimum next neighbor distance of the Cl^- ions is $a = 3.86 \pm 0.15$ Å and is observed for the unit cell marked by the lower/left thick arrow Figure 3 (a). This corresponds to a contraction of $11 \pm 4\%$ with respect to the lattice constant observed on the terraces, while the other unit cells differ by only 1–2% ($\pm 3\%$). Thus, the main distortion (Δx and Δz) in the carpet region is concentrated on only two of the four KCl unit cells in the carpet region. For the growth across Ag triple steps, as illustrated in Figure 3 (b), we observe the same behavior because the step splitting leads to the growth across three distinct mono-atomic Ag steps. In order to visualize the arrangement, similar ion positions with respect to the carpet region in (a) and (b) are indicated by same colors.

Due to the adaption of the width of the Ag micro-terraces discussed above, the Cl^- ions are always close to Ag step edges. Otherwise, we would not be able to interpret the contrast observed in the STM images. For the split triple step in Figure 3 (b), we can describe the situation by three directly adjacent carpet regions. Here, on average, the unit cells marked exemplarily by thick arrows for the upmost carpet region compensate for $42 \pm 9\%$ and $38 \pm 12\%$ (top to bottom), of the height of a mono-atomic Ag step. The two peripheral unit cells marked by the thin arrows contribute with $19 \pm 5\%$,

and hence, again less to the adaption of the KCl lattice to the height difference of the step. Thus, the situation is very similar to the situation observed for the carpet growth across the mono-atomic Ag step discussed above. However, as the carpet growth directly continues across the next step edge, the distributions of the lateral distortion (Δx) is more balanced and the unit cells only differ by a maximum of $\pm 6\%$ from the lattice constant found on the terraces. In both of these situations of carpet growth, across mono-atomic and higher Ag steps, we do not observe a distortion of the unit cells in the direction parallel to the Ag step. However, perpendicular to the step, the projection of the distorted unit cells within the carpet region onto the Ag $\langle \bar{1}\bar{1}2 \rangle$ direction leads to shorter distances. This might allow for the two Cl^- ions which are on the upper and lower terrace adjacent to the carpet growth region (marked by stars), to occupy the same and energetically preferred adsorption sites with respect to the underlying Ag surface as it is visible in Figure 3 (c).

Thus, we are able to present the first atomistic model for the carpet growth of KCl on Ag(111) from which we learn the following: The ionic arrangement of the KCl lattice at the Ag step appears to be related to the step dipole and leads to a preferred growth with the polar KCl $\langle \bar{1}\bar{1}0 \rangle$ lattice lines parallel and perpendicular to the step edge. The distortion of the KCl lattice in the carpet region, necessary to adapt to the height of the next terrace, is however, not distributed uniformly across the width of the involved four KCl unit cells. A possible reason for this could be the attempt of the KCl lattice to adapt to the charge distribution related to the step dipole on the upper and on the lower side of the Ag step edge. This is different from the continuum model for the carpet growth developed by Schwennike et al., who considered a uniform distortion for the NaCl unit cells in the carpet regions on Ge(100).⁸ The distortion of the KCl lattice in x and z direction, which is strongest for the two KCl unit cells indicated by thick arrows in Figure 3, costs energy. On the other hand, the strong, non-uniform

distortion of the KCl layer gains energy as the range in which the KCl layer is lifted away from the metal surface is decreased. In particular, the strong vertical distortion is supportingly favored by the attractive interactions between the step dipole related charges at the lower part of the Ag step edge and the K^+ ions in the KCl layer. In addition, the KCl layer is always attracted by the mirror charges on the Ag terraces. Finally, the strong bending of the carpet growth region resulting in the width of four unit cells, favors the occupation of equal adsorption sites for the two Cl^- ions which are on the upper and lower terrace adjacent to the carpet growth region.

For higher Ag steps an additional loss of energy is avoided by a step splitting of the Ag steps into steps of mono-atomic height. The width of the created micro-terraces is determined by the width of the carpet region and cannot fall below it. This step splitting and the azimuthal reorientation of steps is expected to occur during the deposition and is supported by the elevated sample temperature of 403 K. The increased diffusion of Ag and KCl at this temperature, allowing for the step splitting but still low enough to avoid a dewetting of the Ag surface, thus might be the reason that sample temperatures of about 400 K are ideal for growing closed KCl films on Ag surfaces.²² By these mechanisms, the Ag(111) surface adapts to the KCl layer. This is supported by the high mobility of Ag atoms located at steps or kink sites.^{33,34} The system gains energy by the step splitting of higher Ag steps and by the straightening of the overgrown Ag steps. A similar straightening of Ag(111) step edges was observed for the carpet growth of NaCl/Ag(111) by Matthaëi et al. who performed the deposition at 293–303 K.¹⁴ However, the KCl carpet region observed in our measurements is twice as large as for NaCl (four instead of two AH unit cells)¹⁴ and differently, we also do not observe a reconstruction or a buckling of the KCl layer induced by kink sites of the step edges.³⁵

In summary, our studies of epitaxial KCl(100) layers on the Ag(111) surface demonstrate that

the ion arrangement in the carpet growth region of AH films on metal surfaces is non-uniform and of a defined, short width of, in our case, four KCl unit cells. Hence, the continuum model for the carpet growth of AH as introduced by Schwennike et al.,⁸ is not appropriate here. Instead, models which provide an atomistic description of the ionic arrangement are needed to account for the interactions between the ionic layer and the metal surface, related to the step dipoles, the image charges of the surface, and the possible commensurate arrangement of the AH ions with respect to the metal surface. As these interactions are relevant for all combinations of AH and metal surfaces, although to different extent, this conclusion applies for all AH films on metal surfaces which show a carpet growth behavior. The KCl induced splitting of higher Ag steps into monoatomic steps, made possible by elevated sample temperatures during the deposition, favors the continuous AH growth across the step edges. A direct overgrowth of higher Ag steps does not occur, but the step splitting allows for the growth of the AH domains to continue such that a growth of large domains is enabled. The here presented example for the carpet growth also demonstrates that there is a minimum step width of about 13 Å which is needed for the carpet growth. This is of special importance when the growth on vicinal surfaces with small terrace widths is considered, possibly under the aim to further tune growth modes of organic adsorbates on AH decoupling layers.

Supporting Information Available

Supporting Information: Additional experimental details concerning the layer corrugation and the determination of the KCl lattice constants.

Acknowledgement We thank Callum Hayward, Dylan Barker, Martin Specht, and Morris Mühlpointner for experimental support. The work was funded by the German research foundation (DFG) through the research training

group 2591. A.S. thanks the Royal Society for funding via a University Research Fellowship, and the ERC for funding under Grant Agreement number 757720 3DMOSHBOND.

References

- (1) Repp, J.; Meyer, G.; Stojković, S. M.; Gourdon, A.; Joachim, C. Molecules on Insulating Films: Scanning-Tunneling Microscopy Imaging of Individual Molecular Orbitals. *Phys. Rev. Lett.* **2005**, *94*, 026803.
- (2) Gross, L.; Schuler, B.; Pavliček, N.; Fatayer, S.; Majzik, Z.; Moll, N.; Peña, D.; Meyer, G. Atomic Force Microscopy for Molecular Structure Elucidation. *Angewandte Chemie International Edition* **2018**, *57*, 3888–3908.
- (3) Kaiser, K.; Lieske, L.-A.; J. Repp, J.; Gross, L. Charge-state lifetimes of single molecules on few monolayers of NaCl. *Nat. Commun.* **2023**, *14*.
- (4) Imai-Imada, M.; Imada, H.; Miwa, K. Orbital-resolved visualization of single-molecule photocurrent channels. *Nature* **2022**, *603*, 829–834.
- (5) Illarionov, Y.; Knobloch, T.; Jech, M.; Lanza, M.; Akinwande, D.; Vexler, M.; Müller, T.; Lemme, M.; Fioro, G.; Schwierz, F. et al. Insulators for 2D nanoelectronics: the gap to bridge. *Nature Communications* **2020**, *11*, 3385.
- (6) Hoffmann-Vogel, R. Imaging prototypical aromatic molecules on insulating surfaces: a review. *Reports on Progress in Physics* **2018**, *81*, 016501.
- (7) Bombis, C.; Ample, F.; Lafferentz, L.; Yu, H.; Hecht, S.; Joachim, C.; Grill, L. Single Molecular Wires Connecting Metallic and Insulating Surface Areas. *Angewandte Chemie International Edition* **2009**, *48*, 9966–9970.

- (8) Schwennicke, C.; Schimmelpfennig, J.; Pfnür, H. Morphology of thin NaCl films grown epitaxially on Ge(100). *Surface Science* **1993**, *293*, 57–66.
- (9) Bennewitz, R.; Barwich, V.; Bammerlin, M.; Loppacher, C.; Guggisberg, M.; Baratoff, A.; Meyer, E.; Güntherodt, H.-J. Ultrathin films of NaCl on Cu(111): a LEED and dynamic force microscopy study, journal = Surface Science. **1999**, *438*, 289–296.
- (10) Kramer, J.; Tegenkamp, C.; Pfnür, H. The growth of NaCl on flat and stepped silver surfaces. *Journal of Physics: Condensed Matter* **2003**, *15*, 6473.
- (11) Loppacher, C.; Zerweck, U.; Eng, L. M. Kelvin probe force microscopy of alkali chloride thin films on Au(111). *Nanotechnology* **2003**, *15*, S9.
- (12) Repp, J.; Meyer, G. Scanning tunneling microscopy of adsorbates on insulating films. From the imaging of individual molecular orbitals to the manipulation of the charge state. *Applied Physics A* **2006**, *85*, 399–406.
- (13) Lauwaet, K.; Schouteden, K.; Janssens, E.; Van Haesendonck, C.; Lievens, P.; Trioni, M. I.; Giordano, L.; Pacchioni, G. Resolving all atoms of an alkali halide via nanomodulation of the thin NaCl film surface using the Au(111) reconstruction. *Phys. Rev. B* **2012**, *85*, 245440.
- (14) Matthaei, F.; Heidorn, S.; Boom, K.; Bertram, C.; Safiei, A.; Henzl, J.; Morgenstern, K. Coulomb attraction during the carpet growth mode of NaCl. *Journal of Physics: Condensed Matter* **2012**, *24*, 354006.
- (15) Bera, A.; Morgenstern, K. In Situ Growth and Bias-Dependent Modification of NaBr Ionic Layers on Ag(111). *The Journal of Physical Chemistry C* **2022**, *126*, 10610–10617.
- (16) Repp, J.; Fölsch, S.; Meyer, G.; Rieder, K.-H. Ionic Films on Vicinal Metal Surfaces: Enhanced Binding due to Charge Modulation. *Phys. Rev. Lett.* **2001**, *86*, 252–255.
- (17) Kiguchi, M.; Entani, S.; Saiki, K.; Inoue, H.; Koma, A. Two types of epitaxial orientations for the growth of alkali halide on fcc metal substrates. *Phys. Rev. B* **2002**, *66*, 155424.
- (18) Glöckler, K.; Sokolowski, M.; Soukopp, A.; Umbach, E. Initial growth of insulating overlayers of NaCl on Ge(100) observed by scanning tunneling microscopy with atomic resolution. *Phys. Rev. B* **1996**, *54*, 7705–7708.
- (19) Weast, R. C., Ed. *Handbook of Chemistry and Physics*, 55th ed.; CRC Press, Cleveland, 1974.
- (20) Smoluchowski, R. Anisotropy of the Electronic Work Function of Metals. *Phys. Rev.* **1941**, *60*, 661–674.
- (21) Müller, M.; Ikononov, J.; Sokolowski, M. Structure of Epitaxial Layers of KCl on Ag(100). *Surface Science* **2011**, *605*, 1090–1094.
- (22) Mühlpointner, M. E. L. Investigations on the Growth of KCl-Films on the Ag(100) Surface via SPA-LEED. Bachelor's thesis, Rheinische Friedrich-Wilhelms Universität Bonn, 2021.
- (23) Bretel, R.; Le Moal, S.; Oughadou, H.; Le Moal, E. Hydrogen-bonded one-dimensional molecular chains on ultrathin insulating films: Quinacridone on KCl/Cu(111). *Phys. Rev. B* **2023**, *108*, 125423.
- (24) Hambling, P. J. The lattice constants and expansion coefficients of some halides. *Acta Cryst.* **1953**, *6*, 98.
- (25) Barrett, W. T.; Wallace, W. E. Studies of NaCl-KCl Solid Solutions. I. Heats of Formation, Lattice Spacings, Densities,

- Schottky Defects and Mutual Solubilities. *Journal of the American Chemical Society* **1954**, *76*, 366–369.
- (26) Kantola, M. X-ray studies on the thermal expansion of solid solutions of KCl and KBr. *VTT Technical Research Centre of Finland* **1947**, *3*, 12.
- (27) Walker, D.; Verma, P. K.; Cran-
swick, L. M.; Jones, R. L.; Clark, S. M.;
Buhre, S. Halite-sylvite thermoelasticity.
American Mineralogist **2004**, *89*, 204–
210.
- (28) Humberg, N.; Guo, Q.; Bredow, T.;
Sokolowski, M. Growth of Hydrogen-
Bonded Molecular Aggregates on a Thin
Alkali Halide Layer: Quinacridone on
KCl/Ag(100). *The Journal of Physical
Chemistry C* **2023**, *127*, 23814–23826.
- (29) Li, Z.; Schouteden, K.; Iancu, V.;
Janssens, E.; Lievens, P.; Hae-
sendonck, C. V.; Cerdá, J. I. Chemically
modified STM tips for atomic-resolution
imaging of ultrathin NaCl films. *Nano
Res.* **2015**, *8*, 2223–2230.
- (30) Smakula, A.; Kalnajs, J. Precision De-
termination of Lattice Constants with
a Geiger-Counter X-Ray Diffractometer.
Phys. Rev. **1955**, *99*, 1737–1743.
- (31) Straumanis, M. E. Neubestimmung der
Gitterparameter, Dichten und thermis-
chen Ausdehnungskoeffizienten von Silber
und Gold, und Vollkommenheit der Struk-
tur. *Mh. Chem.* **1971**, *102*, 1377–1386.
- (32) Majee, R.; Kumar, A.; Das, T.;
Chakraborty, S.; Bhattacharyya, S.
Tweaking Nickel with Minimal Silver
in a Heterogeneous Alloy of Decahedral
Geometry to Deliver Platinum-like Hy-
drogen Evolution Activity. *Angewandte
Chemie International Edition* **2020**, *59*,
2881–2889.
- (33) Wolf, J.; Vicenzi, B.; Ibach, H. Step
roughness on vicinal Ag(111). *Surface Sci-
ence* **1991**, *249*, 233–236.
- (34) Poensgen, M.; Wolf, J.; Frohn, J.;
Giesen, M.; Ibach, H. Step dynamics on
Ag(111) and Cu(100) surfaces. *Surface
Science* **1992**, *274*, 430–440.
- (35) Heidorn, S.; Gerss, B.; Morgenstern, K.
Step Edge Induced Reconstructions of
NaCl(100) Bilayers on Ag(111): A Route
To Alter the Properties of Nanoscale In-
sulators. *ACS Applied Nano Materials*
2018, *1*, 6818–6823.